



# Three-dimensional individual planning for treatment of ameloblastoma of the mandible – clinical study

Krystian Kuźniarz<sup>1,A-D</sup>, Elżbieta Kwiatkowska<sup>1,A,C-D</sup>, Remigiusz Czerkies<sup>1,A-C</sup>,  
Agnieszka Lasota<sup>2,E-F</sup>, Jadwiga Sierocińska-Sawa<sup>3,C,E</sup>, Tomasz Tomaszewski<sup>1,E-F</sup>

<sup>1</sup> Department and Clinic of Maxillofacial Surgery, Medical University, Lublin, Poland

<sup>2</sup> Chair and Department of Jaw Orthopaedics, Medical University, Lublin, Poland

<sup>3</sup> Department of Pathology, Independent Public University Hospital No. 1, Lublin, Poland

A – Research concept and design, B – Collection and/or assembly of data, C – Data analysis and interpretation, D – Writing the article, E – Critical revision of the article, F – Final approval of the article

Kuźniarz K, Kwiatkowska E, Czerkies R, Lasota A, Sierocińska-Sawa J, Tomaszewski T. Three-dimensional individual planning for treatment of ameloblastoma of the mandible – clinical study. J Pre-Clin Clin Res. 2023; 17(3): 198–207. doi: 10.26444/jpccr/170251

## Abstract

Ameloblastoma is the odontogenic tumour of the maxillary bones accounts for approximately 1% of all dental tumours. It is clinically considered to be a lesion with local aggressiveness and a high level of tendencies to relapse, destruction of surrounding tissues, and even malignancy and metastases. The treatment of choice is currently the resection of bone *en bloc* with a 1–2 cm margin of healthy tissue along with its simultaneous reconstruction. Newly introduced technologies are beginning to play an increasingly important role in modern head and neck surgery. Virtual surgical planning using 3D models (CAD) allows individualised (CAM) custom-made guides and titanium prosthesis, which constitutes the individualisation of treatment. The case report presents a patient treated due to ameloblastoma of the body of the mandible, with deep circumflex iliac artery flap (DCIAF) reconstruction using elements of individual 3D planning.

## Key words

Ameloblastoma, CAD/CAM, Iliac crest flap

## INTRODUCTION

Ameloblastoma (AM) is a odontogenic tumour of the maxillary bones originating from the epithelial remains of the odontogenic organ. Despite its benign histopathological nature, it is clinically considered to be a lesion with local aggressiveness and a high level of tendencies to relapse, destruction of surrounding tissues, and even malignancy and metastases [1, 2]. The latest classification of dental tumours proposed by the WHO in 2022 not only modified the current position regarding its histological types, but also introduced a newly-defined hybrid lesion with a component typical of AM, called the adenoid ameloblastoma (Fig. 1) [3, 4]. Due to the nature of the lesion, the current treatment of choice is resection of bone *en bloc* with a 1–2 cm margin of healthy tissue, along with its simultaneous reconstruction to restore lost tissues and the function of the stomatognathic system [5].

Planning a surgical procedure can pose a challenge for the therapeutic team. This is due not only to the extent of the operation, the planned reconstruction, but above all to the specificity of the head and neck area resulting from the complex anatomical structure and a wide range of functions that are important for the entire organism [6]. Three-dimensional surgical planning offers a helpful tool in meeting the above requirements. It is mainly based on close cooperation between the surgical team and the biomedical engineer, which results in the preparation of individual diagnostic models, surgical guides, and titanium

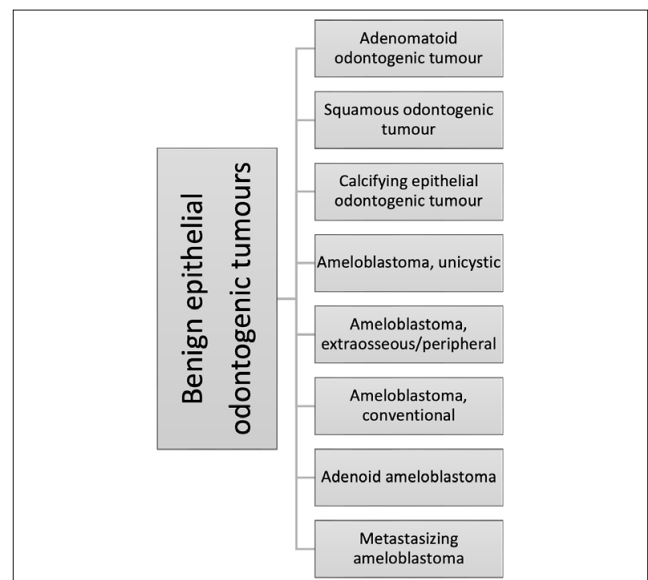


Figure 1. Benign epithelial odontogenic tumours. Fragment of 2022 WHO classification of odontogenic tumours and cysts of jaws

implants based on computer tomography (CT) imaging. The use of these tools brings a number of benefits, i.e. it facilitates the determination of resection limits, which undoubtedly affects the radicality of the procedure and the accuracy of the reconstruction, as well as shortening the time of the surgery, which is of great importance especially for elderly patients or patients burdened with general comorbidities [7].

The study presents the case of a patient, who underwent surgery due to AM of the body of the left mandible with the

✉ Address for correspondence: Krystian Kuźniarz, Department and Clinic of Maxillofacial Surgery, Medical University, Lublin, Poland  
E-mail: krystian.kuzniarz@umlub.pl

deep circumflex iliac artery flap (DCIAF) reconstruction, using elements of individual 3D planning and custom-made design/computer assisted manufacturing (CAD/CAM) guides and titanium prosthesis with 44 months follow-up.

## CASE REPORT

A 48-year-old patient was referred to the Maxillofacial Surgery Clinic due to pain ailments, which had been increasing for several weeks and swelling of the mandibular body in the area of the left premolars teeth. The performed pantomographic image revealed the presence of a multi-locular lesion of the mandibular body in the area of teeth 33–35. After a biopsy sample collected for histopathological examination, *follicular ameloblastoma* was diagnosed. At admission, the patient's physical examination revealed a slight swelling of the cheek and lower lip on the left side, distension of the mandible particularly marked on the vestibular side and pathological, II° mobility of tooth 33, which resulted in shallowing of the bottom of the vestibule of the oral cavity in the projection of the lesion, and discomfort during palpation. With the exception of arterial hypertension, no other diseases were diagnosed.

In order to more accurately assess the afore-described lesion, the imaging diagnostics was extended to include craniofacial CT scan with contrast. Diagnostics performed at the II Department of Medical Radiology of the Independent Public Clinical Hospital No. 1 in Lublin (0.625 mm layers) demonstrated the presence, in the left mandibular body, from the level of the root of tooth 31 to the area of tooth 36, of a well-delineated multilocular lesion, subject to slight contrast enhancement, sized approx. 37×17×25 mm (AP×LR×CC). At this level, the examination revealed a small bone distension with segmental thinning and destruction of the cortical layer on both the vestibular and lingual sides, as well as partial resorption of the root of tooth 33 (Figs. 2–4).

Based on the clinical image, radiological scans and the microscopic examination result, the patient was qualified for segmental resection of the mandibular body from the 43/44 area to the height of the anterior margin of the mandibular ramus, including the lesion and a margin of healthy tissue. At the same time, a simultaneous reconstruction of the lost tissues with a DCIAF was planned (Fig. 5). The pelvic CT performed at the II Department of Medical

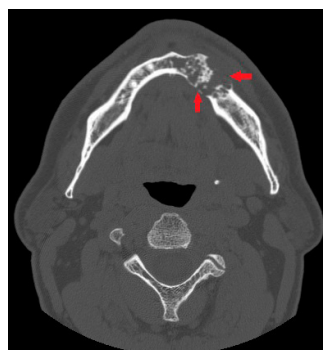


**Figure 2.** CT scan. Horizontal cross-section. Multilocular lesion (red arrows) of the ameloblastoma type of the mandibular body of the 31–36 region

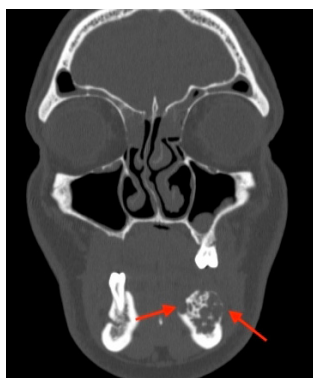


**Figure 3.** CT scan. AP cross-section. A lesion of the mandibular body with the character of an ameloblastoma. Visible destruction of the vestibular and lingual cortical plate (red arrows)

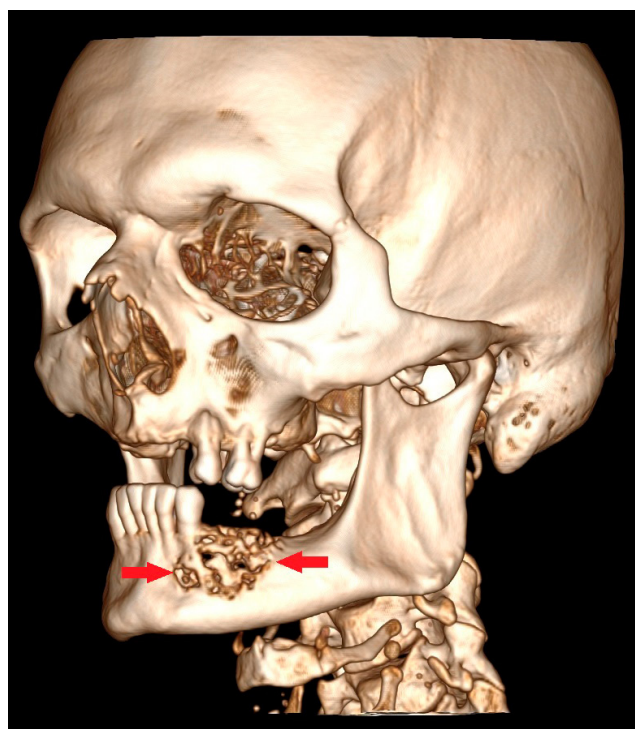


**Figure 4.** 3D computer tomography reconstruction. The red arrows indicate the direction of the greatest expansion of the ameloblastoma lesion within the left mandibular body

Radiology of the Independent Public Clinical Hospital No. 1 in Lublin allowed for assessment of the donor site of the planned transplant (1.25 mm layers). Based on the imaging examinations performed, three-dimensional, individual planning of the surgical procedure was initiated, along with the implementation of custom-made CAD/CAM guides and titanium prosthesis in cooperation with biomedical engineers from the ChM Poland company.

Planning the surgery was started with stereolithographic 3D models of both the mandible and a fragment of the iliac crest (Figs. 6–8). In the next stage, based on the performed radiological diagnostics and prepared models, custom-made guides were made to determine the locations of the previously planned mandibular resection (Figs. 6 and 7). In addition, based on the assessment of the volume, size and shape of the mandibular fragment qualified for resection, osteotomy in the area of the left iliac crest was planned, which would allow for accurate reconstruction of the lost mandibular body fragment and for this purpose, an appropriate custom-made guide was also executed (Figs. 8 and 9). Then, a 3D computer simulation of the expected effect of the surgical procedure was carried out (Fig. 10) and an individual titanium prosthesis was designed and constructed to fuse the bone flap with the remaining fragments of the mandible. Earlier drilling at the stage of using guides allowed for its precise positioning in relation to the mandible and joining it in the previously planned position without making additional, new holes for connecting screws (Fig. 11).

Two surgical teams performed the planned surgery under general anesthesia. The first team performed a segmental resection of the mandibular body to the extent determined by the prepared guides. At the same time, the second surgical team took a free flap covering a fragment of the iliac crest marked by surgical guide, the internal oblique muscle along

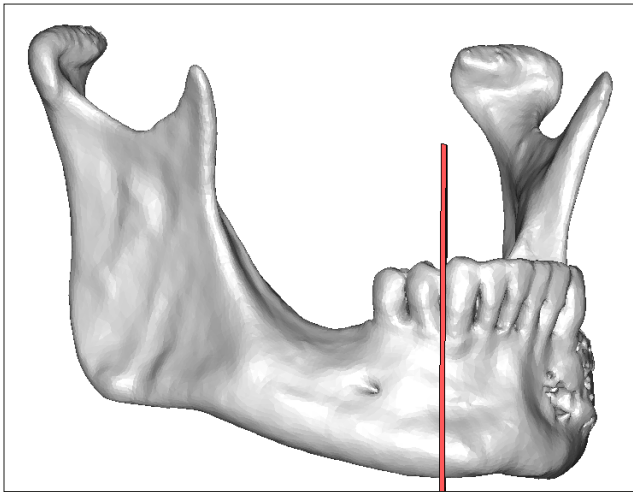


**Figure 5-A.** Individual planning of 3D surgery. Images based on CT examination. Planned osteotomy site on the right side in the area of 43/44 tooth marked with a red line

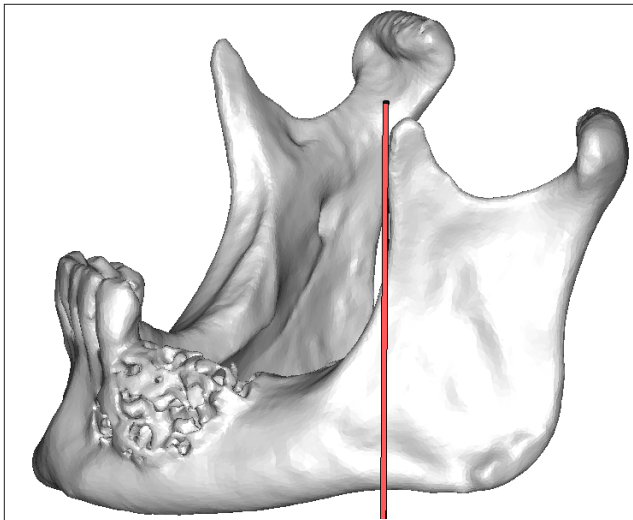


**Figure 5-B.** Planned osteotomy site on the left side, tangential to the anterior margin of the mandibular ramus marked with a red line

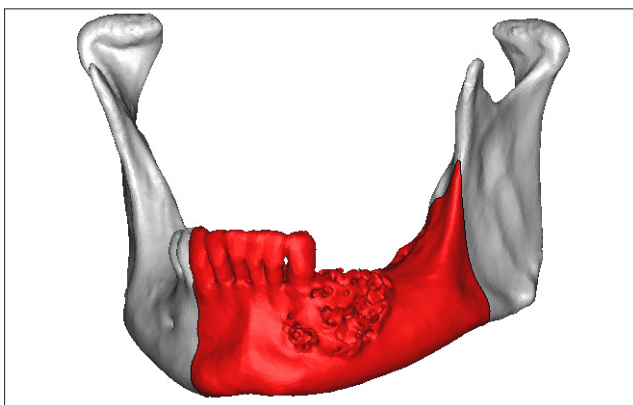


**Figure 5-C.** The scope of the planned mandibular resection marked in red

with a vascular pedicle composed of the deep circumflex iliac vessels to the extent previously determined. After insertion of the flap into the recipient site in the oral cavity, vascular microanastomosis end-to-end between the facial artery and the deep circumflex iliac artery was performed. Next, venous vessels anastomosis was performed using a 3.5 mm vascular coupler (Synovis Micro Companies Alliance, INC). The bony

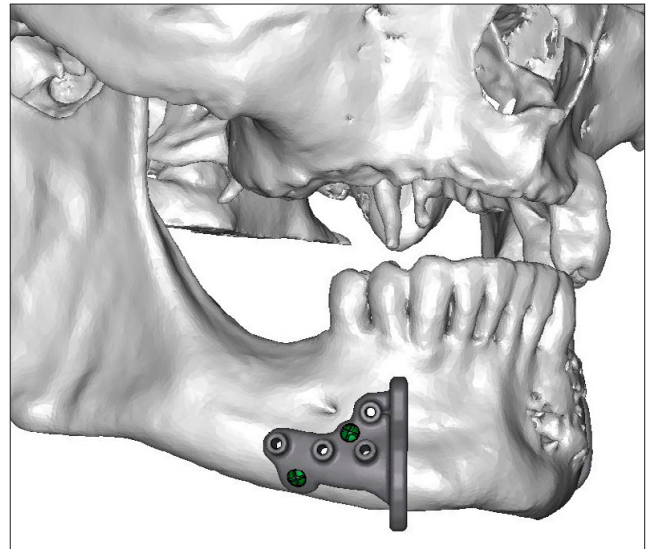


**Figure 6-A.** Planning stage. 3D image based on CT scan. Visible design of a custom-made guide marking the location of osteotomy on the right side. Titanium screws (green) guaranteeing the stability of the guide during osteotomy were marked. The remaining holes defining the drilling locations were used in subsequent stages of the surgery



**Figure 6-B.** Diagnostic model of the mandible with a guide for osteotomy on the right side

part of the flap was fixed to the mandible with the help of the individually prepared titanium prosthesis, and the muscular part was used to fill the tissue loss in the left submandibular space (Fig. 12). The wounds in the area of the mouth and neck were treated in layers from edge-to-edge.

A follow-up X-ray image showing normal mandibular body reconstruction is shown in Figure 13. Histopathological examination of the surgical preparation confirmed the previous diagnosis, at the same time determining the radicality of the performed resection (Fig. 14).

On day 7 after the surgery, a dehiscence of the post-operative wound in the oral cavity was observed in the anterior part of the graft providing the bone fragment of the DCIAF with normal blood supply (Fig. 15-A). Emergency provision of the resulting dehiscence with surgical stitches did not produce the expected results, which necessitated further dehiscence of the wound and exposure of the mini plate of this area (Fig. 15-B).

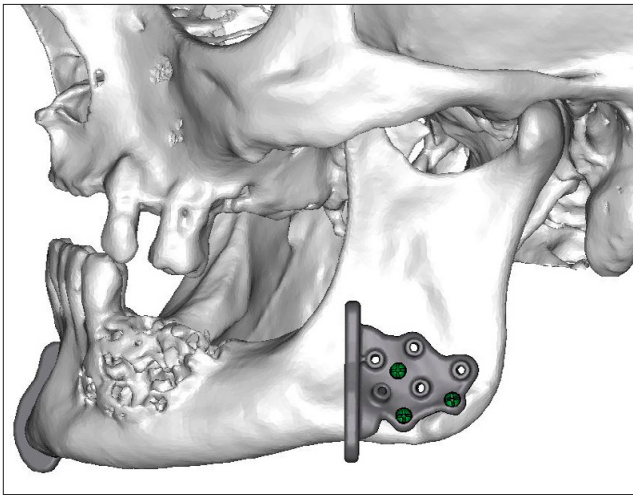


**Figure 7-A.** Planning stage. 3D image based on CT scan. Visible design of a custom-made guide marking the location of osteotomy on the left side. Titanium screws (green) guaranteeing the stability of the guide during osteotomy are marked. The remaining holes defining the drilling locations were used in subsequent stages of the surgery

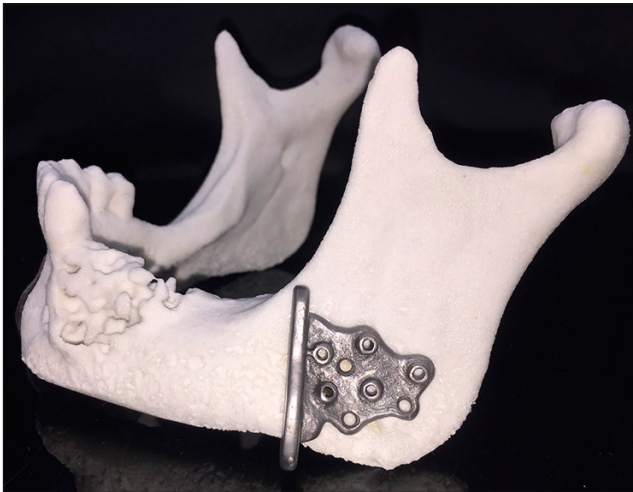


**Figure 7-B.** Diagnostic model of the mandible with a guide for osteotomy on the left side

During this time, the patient was fed extraorally with a nasogastric tube, and dressings were used to promote wound epithelialization.

The dehiscence was qualified for secondary healing by granulation, and its subsequent stages are shown in Figure 15. The presence of symptoms of local inflammation of the 33–43 dental area were found during subsequent follow-up examination carried out 6 months after surgery. A revision of the above-mentioned area was performed with intraoral access under general anaesthesia. Full fusion of bones and unstable single, loose splicing screws were found, which were removed together with the plate (Fig. 16). In the follow-up period of 44 months, no disturbing symptoms or features of recurrence of the pathological process were observed in either the clinical or radiological examinations (Figs. 17 and 18).

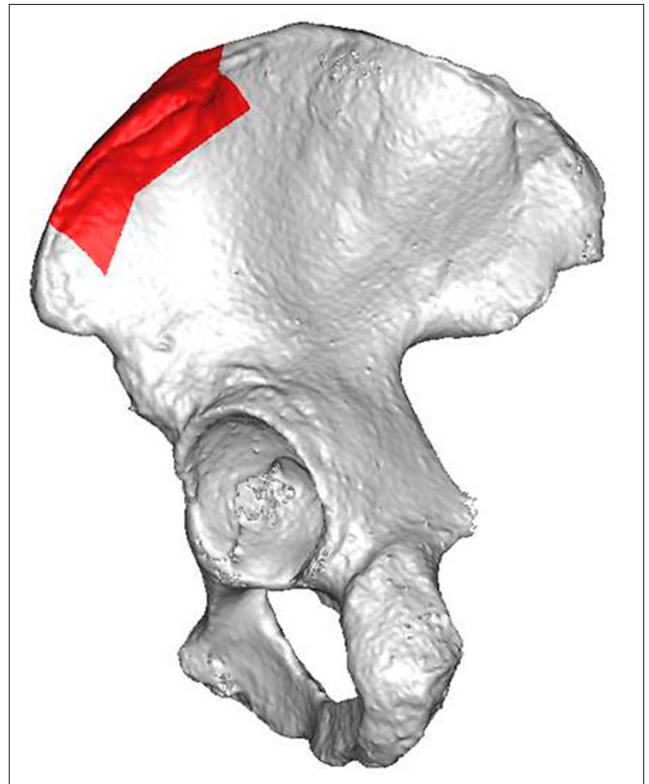


**Figure 8-A.** Individual planning of 3D surgery. Images based on CT examination. The planned extent of osteotomy in the left iliac wing is marked in red. Lateral view

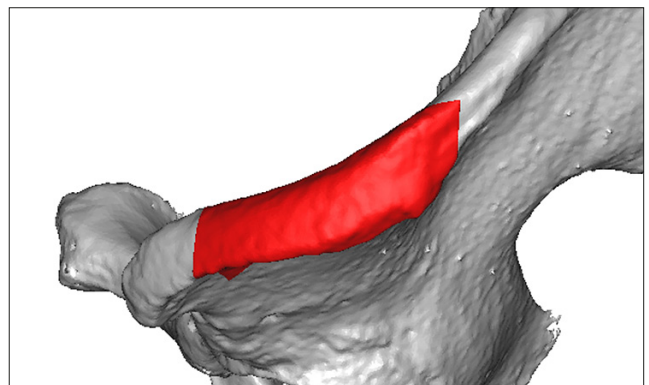


**Figure 8-B.** Top view

## DISCUSSION

AM accounts for approximately 1% of all dental tumours [8]. The most common location is the area of the molars teeth and the angle of the mandible, which are responsible for up to 70% of cases [9]. The lesion is most often observed in patients in the 4th decade of their life, regardless of gender. Frequently, the initial neoplastic process is asymptomatic and such cases are detected on the basis of routinely taken X-ray images. The first symptoms indicating the ongoing pathological process include: bone distension, pathological tooth mobility, malocclusion, facial asymmetry, and emerging pain; signs of inflammation may indicate the presence of a pathological fracture [10, 11].

As reported by Alves et al., CT with contrast enhancement should be the examination of choice to assess the location of the lesion and its extent [12]. Although initially AM can

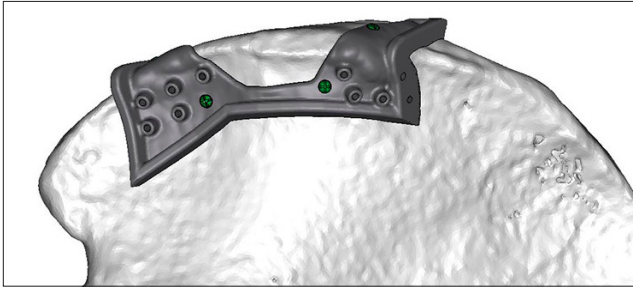


Figure 9-A. Planning stage. 3D image based on CT scan. Visible custom-made guide design determining the place of osteotomy in the iliac crest. Lateral view

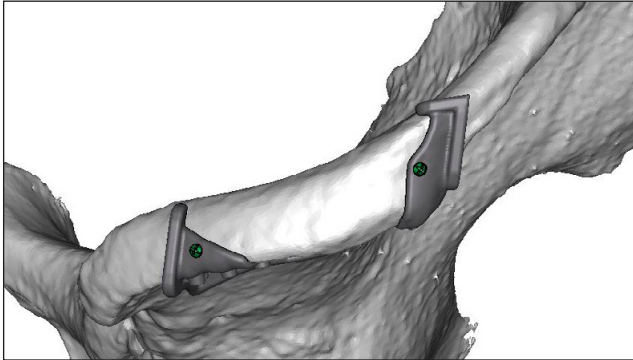


Figure 9-B. Top view. Titanium screws (green) guaranteeing the stability of the guide during osteotomy are marked. The remaining holes defining the drilling locations were used in subsequent stages of the surgery



Figure 9-C. Diagnostic model of a fragment of the iliac crest with a guide for its osteotomy

develop asymptotically between the compacted bone plates, in subsequent stages it leads to their distension, modelling, and often also complete destruction of the cortical

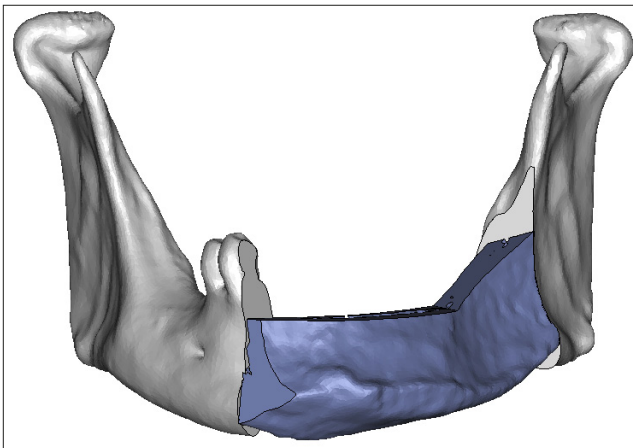


Figure 10-A. 3D simulation of the expected effect of mandibular surgery. The introduced fragment of ilium is marked in blue. AP view

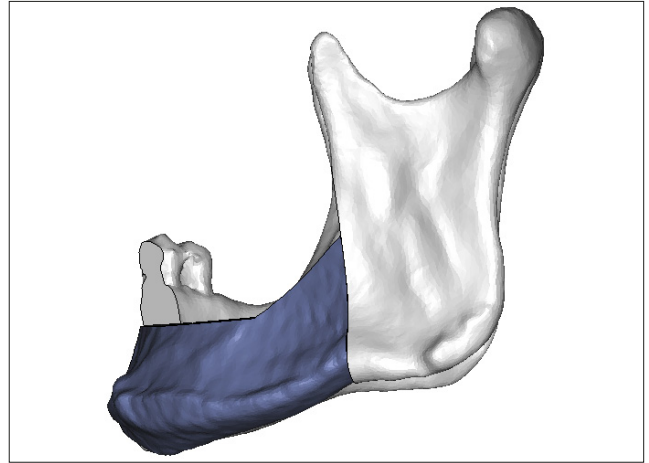


Figure 10-B. Lateral view

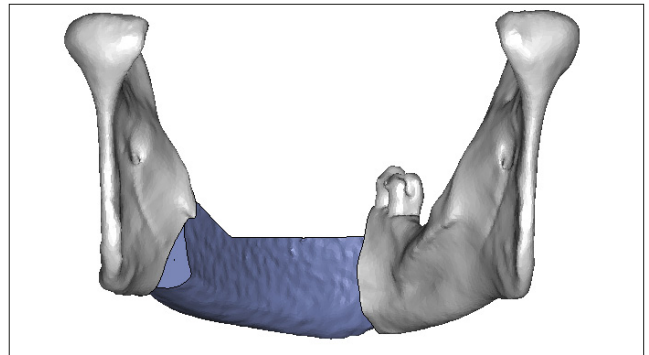


Figure 10-C. PA view

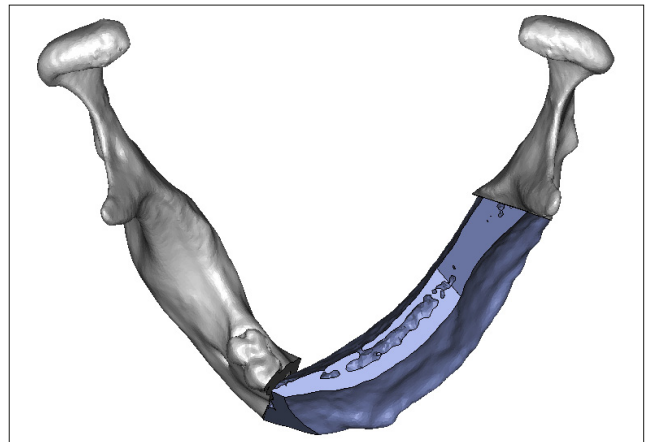


Figure 10-D. Top view

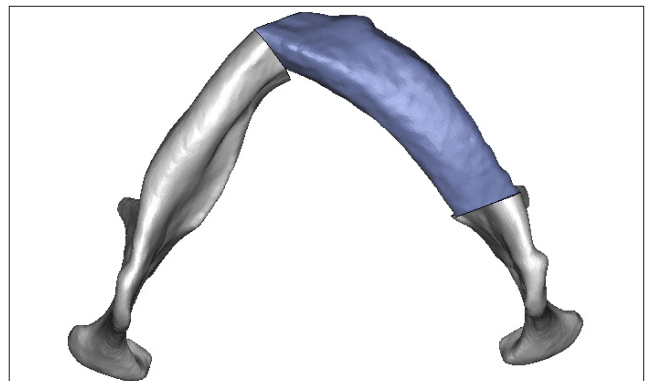
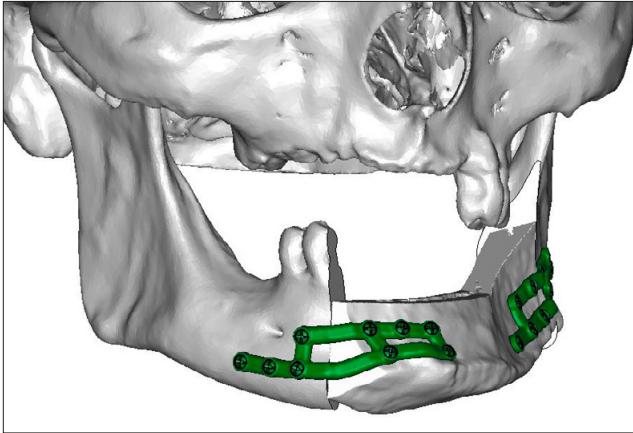
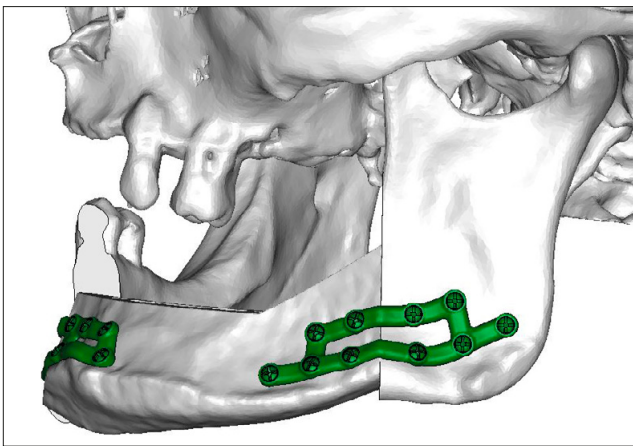


Figure 10-E. Bottom view



**Figure 11-A.** Design of individual titanium prosthesis as elements connecting the flap with the mandible. AP view



**Figure 11-B.** Lateral view

plate on both the vestibular and lingual sides in the case of the advanced disease process [13]. Studies indicate that up to 70% of lesions present a radiological image of well-delimited multi-locular radiolucency with the presence of more saturated septa within it. In the literature, this



**Figure 12.** Intra-operative image. Condition after segmental resection of the mandible with removal of the left submandibular salivary gland and the adjacent lymph nodes. Visible anastomotic fragment of the DCIAF with the remaining fragments of the mandible and the internal oblique muscle filling the submandibular space of the left side. Condition after vascular microsurgery and normal reperfusion of flap elements



**Figure 13.** Follow-up X-ray after surgery. Visible fragment of the iliac bone wing fused to the remaining mandibular fragments using individual titanium prosthesis

characteristic image is called soap-bubble appearance or honeycombed pattern, depending on the size of the resulting chambers. Despite the fact that the multi-locular image of the tumor is also visible on classic pantomographic images, only CT examination allows assessment of the extent of the lesion and possible destruction of surrounding tissues. AM-surrounded teeth usually undergo displacement, but pathological root resorption of the teeth is also observed in some cases [14].

The aggressive nature of AM is evidenced by high relapse rates reaching 90.9% in the case of conservative treatment (marsupialization, enucleation, curettage), and

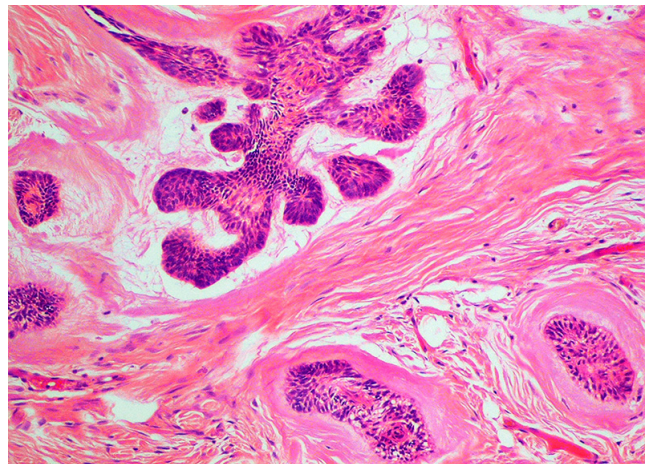


**Figure 14-A.** Microscopic image of the resected tumour. Haematoxylin and eosin staining. Basaloid pattern of ameloblastoma

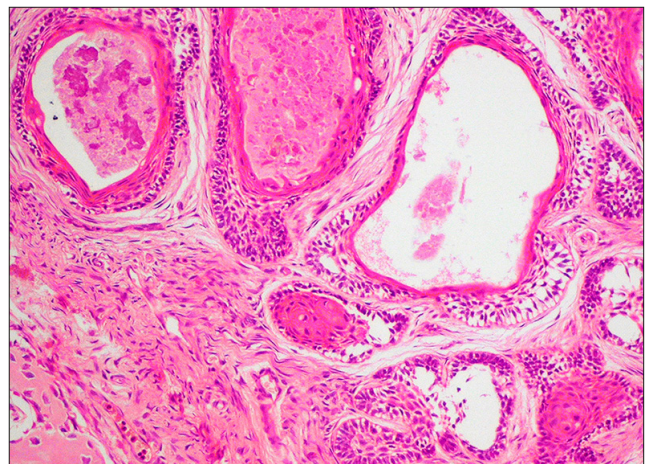


**Figure 14-B.** Peripheral palisading and central stellate reticulum areas



Figure 15-A. Oral cavity wound dehiscence 7 days after surgery



Figure 15-B. Exposure of the connecting plate 14 days after surgery



Figure 15-C. Subsequent stages of secondary healing in the oral cavity 19 days after surgery



Figure 15-D. Subsequent stages of secondary healing in the oral cavity 22 days after surgery



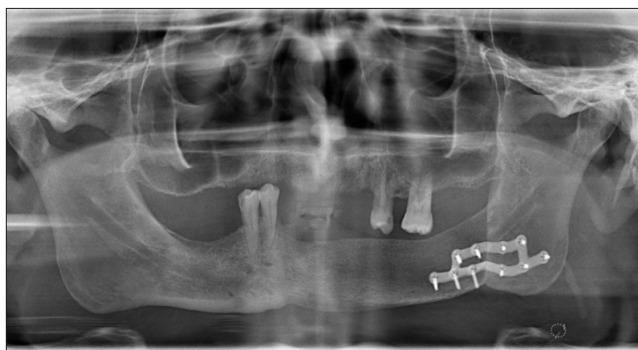
Figure 15-E. Subsequent stages of secondary healing in the oral cavity 25 days after surgery



Figure 15-F. Subsequent stages of secondary healing in the oral cavity 28 days after surgery



Figure 15-G. Subsequent stages of secondary healing in the oral cavity 3 months after the surgery



**Figure 16.** X-ray image taken 6 months after surgery, after removal of the anastomosis of the tooth area 33–43. Visible complete bone healing between the flap and mandibular bone

9.1% in the case of radical treatment (segmental resection). The authors also point to the risk of malignancy or distant metastases, most often to the lungs, especially in the absence of radicality of procedure [15]. Such features require decisive action in the form of segmental bone resection with a healthy tissue margin of 1.5–2 cm, as recommended by most authors [1, 2, 6, 7, 9, 10, 13, 15, 16]. In addition, numerous studies indicate that cortical plate destruction sites where the tumour is in direct contact with soft tissues may be predisposed to recurrence. Therefore, it is recommended to remove also the periosteal and even the mucous membrane covering the lesion in these areas [16–18]. The effect of striving to achieve the full radicality of the procedure is the formation of extensive tissue defects and functional disorders in the form of speech, food intake, and swallowing disorder, but also the deterioration of the aesthetic effect of the craniofacial area [16,19,20]. The main objective of AM treatment is their effective, radical removal along with the restoration of the functions of the stomatognathic system and the restoration of satisfactory facial aesthetics [21]. Currently, most authors consider, in addition to ablative treatment, the simultaneous reconstruction of tissues with a free complex flap to constitute the gold standard in the treatment of this pathology [22, 23]. Most clinicians recommend the use of DCIAF or free fibula flap (FFF) [23]. Lonie et al. and Cariati et al. indicate the numerous advantages of DCIAF, i.e. natural, bent shape, adequate height and volume of the bone used for mandibular reconstruction and the possibility of collecting the skin island,



**Figure 17-A.** Oral cavity images during the observation period of the patient 10 months after surgery

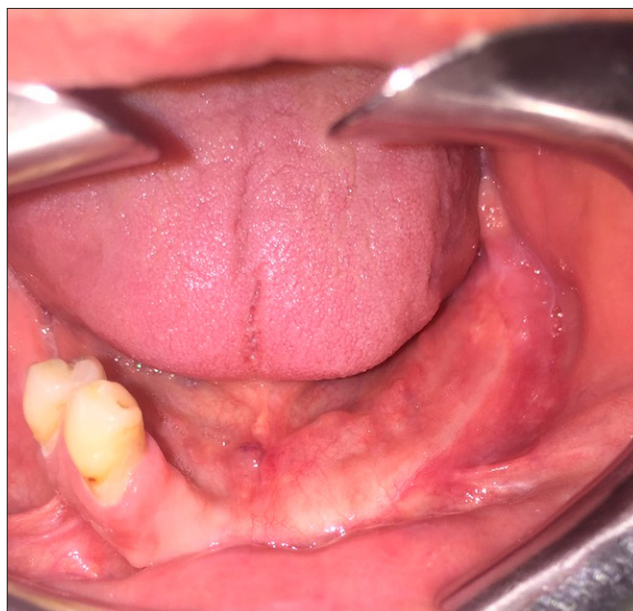


**Figure 17-B.** Oral cavity images during the observation period of the patient 22 months after surgery

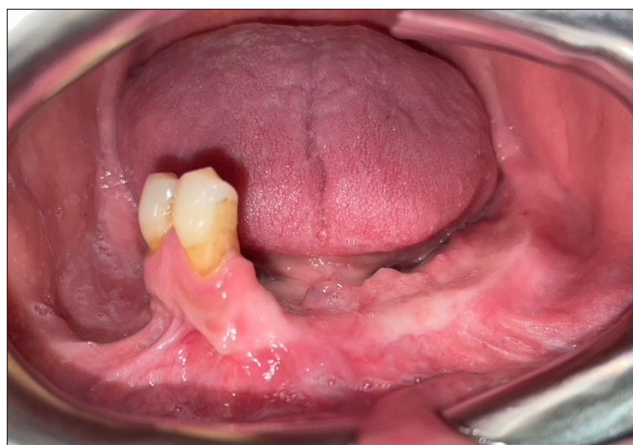


**Figure 17-C.** Oral cavity images during the observation period of the patient 44 months after surgery



**Figure 17-D.** Prosthetic denture used by the patient

as well as the internal abdominal oblique muscle in extensive and complex defects. Nevertheless, it is believed that this flap is technically more difficult to prepare compared to FFF and there is a risk of a herniation in the post-operative wound [23, 24]. Oteri, in turn, recommends FFF, despite the relatively low

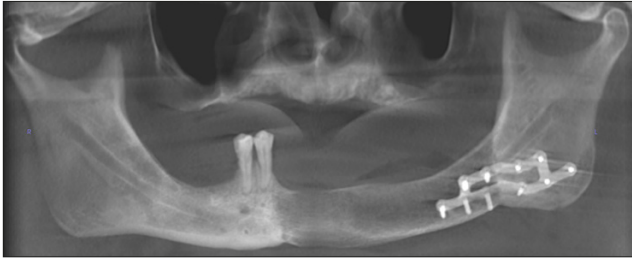


**Figure 18.** X-ray image taken 44 months after surgery. No radiological features of tumor recurrence

height of the bone part of the flap. It also emphasizes the length of the vascular pedicle (average 9 cm) distinguishing this flap, and the length of the transplanted bone (approximately 20 cm), which can be subjected to additional osteotomies to reconstruct more complex mandibular defects, which also determines the presence of double periosteal and medullary blood supply [25–27].

The newly-introduced technologies are beginning to play an increasingly important role in modern head and neck surgery. Virtual surgical planning using 3D models (CAD) allows to execute individualised (CAM) custom-made guides and titanium prosthesis, which constitutes the individualisation of treatment, or made-to-measure surgery. This can improve the accuracy of both resection and reconstructive treatment and contribute to satisfactory aesthetic effects of conducted procedure, thus allowing the patient to maintain their quality of life [28]. Moro et al. describe the use of these tools in the treatment of patients with giant AM with FFF flap reconstruction. However, due to the extent of the disease process, the authors did not have the opportunity to perform classic custom-made guides – due to significantly changed anatomy and the lack of useful anatomical points for their application. They decided to produce a plaster model of the upper dental arch and prosthetic denture of the lower arch with reference to the upper dental arch being a guide for the reconstruction stage. Researchers agree that 3D planning significantly reduces the time of the procedure, as well as improving its precision, both aesthetic and functional effects, despite the above-mentioned limitations of this method [6]. The study presented by Sannomiya et al. also draws attention to the above advantages of this method. In the treatment of mandibular AM, the authors used exclusively bio-models created on the basis of imaging examinations, used for both resection and collection of the bone flap for simultaneous reconstruction. They emphasize the undeniable advantage of this method in the form of shortening the time of the procedure and thus improving the general condition of the patient following this extensive and long surgery [29]. However, the models themselves indicate the scope of individual stages of the procedure only indicatively and do not allow to transfer earlier plans to the surgical field and clearly indicate, for example, the bone osteotomy line. The use of surgical guides solves this problem and makes the procedure more accurate by eliminating the need, often repeated, to trim fragments of the bone flap to the resulting oral cavity defect.

Surgical navigation may constitute another element improving the work of the surgical team. Yu et al. describe the use of virtual planning and surgical guides in the treatment of mandibular AM with DCIAF reconstruction assisted by navigation. Clinicians believe that this method

conditions the direct monitoring of the mandibular position, which contributes to the improvement of the functional and aesthetic effects of this procedure [30]. All authors clearly indicate the benefits of virtual, individual planning of ablative and reconstructive treatment. However, most studies do not assess the post-operative precision of the procedure performed in relation to virtual osteotomies performed at the planning stage. In other words, it is necessary to answer the question whether the prepared individual guides allow for such a range of resection or collection of such a volume of the bone flap, as was assumed at the planning stage of the procedure.

The results of comparative studies indicate that the average error between virtual osteotomy and actual mandibular osteotomy is  $2.06 \pm 0.86$  mm. In addition, the mean error volume between virtual harvested grafts and actual harvested grafts was  $9.12\% \pm 2.84\%$  [31]. The use of virtual planning also translates into the economic aspect of hospital treatment. The introduction of this useful tool into clinical practice is associated with greater involvement of the surgical team in the planning of the procedure and the additional cost that must be incurred. Nevertheless, studies indicate that due to the shortening of the procedure time and the required patient hospitalization time, there was no negative impact on the total cost of treatment of these patients compared to the group of patients treated in a traditional way [32].

In cases of patients with serious general conditions or contraindications to the collection of free flaps, the alternative in the reconstruction of post-resection defects of the mandible seems to be individual, titanium alloplastic implants that faithfully reproduce the geometry of the lost mandible tissue. The surgical guides used in these procedures not only improve the precision of the procedure, but also allow for accurate adhesion and stabilization of the subsequent titanium implant [9]. In turn, subsequent research indicates possible complications associated with the implantation of such extensive titanium implants. The implant may become exposed during radiotherapy in patients originally treated for oral squamous cell carcinoma [7].

## CONCLUSION

Virtual planning of surgical procedures using 3D surgical guides and bio-models is a valuable method for treating patients requiring mandibular resection with simultaneous reconstruction of the free flap. Individualization of treatment allows not only improvement in the precision of osteotomy, but also has a significant impact on the radicality of the procedure, restoration of lost functions of the stomatognathic system, and also leads to the preservation of facial aesthetics, as confirmed in the presented multi-disciplinary procedure.

## REFERENCES

1. Kreppel M, Zöller J. Ameloblastoma-Clinical, radiological, and therapeutic findings. *Oral Dis.* 2018 Mar;24(1–2):63–66. doi:10.1111/odi.12702. PMID: 29480593
2. Effiom OA, Ogundana OM, Akinshipo AO, Akintoye SO. Ameloblastoma: current etiopathological concepts and management. *Oral Dis.* 2018 Apr;24(3):307–316. doi:10.1111/odi.12646
3. Soluk-Tekkesin M, Wright JM. The World Health Organization Classification of Odontogenic Lesions: A Summary of the Changes

- of the 2022 (5th) Edition. *Turk Patoloji Derg.* 2022;38(2):168–184. doi:10.5146/tjpath.2022.01573
4. Jayasooriya PR, Abeyasinghe WAMUL, Liyanage RLPR, Uthpali GN, Tilakaratne WM. Diagnostic Enigma of Adenoid Ameloblastoma: Literature Review Based Evidence to Consider It as a New Sub Type of Ameloblastoma. *Head Neck Pathol.* 2022 Jun;16(2):344–352. doi:10.1007/s12105-021-01358-w
  5. McClary AC, West RB, McClary JR, Fischbein NJ, Holsinger CF, Sunwoo J, Colevas AD, Sirjani D. Ameloblastoma: a clinical review and trends in management. *Eur Arch Otorhinolaryngol.* 2016 Jul;273(7):1649–61. doi:10.1007/s00405-015-3631-8
  6. Moro A, Pelo S, Gasparini G, Saponaro G, Todaro M, Pisano G, D'Amato M, Doneddu P. Virtual Surgical Planning for Reconstruction of Giant Ameloblastoma of the Mandible. *Ann Plast Surg.* 2020 Jul;85(1):43–49. doi:10.1097/SAP.0000000000002390
  7. Cortese A, Spirito F, Claudio PP, Lo Muzio L, Ruggiero A, Gargiulo M. Mandibular Reconstruction after Resection of Ameloblastoma by Custom-Made CAD/CAM Mandibular Titanium Prosthesis: Two Case Reports, Finite Element Analysis and Discussion of the Technique. *Dent J (Basel).* 2023 Apr 20;11(4):106. doi:10.3390/dj11040106
  8. Neagu D, Escuder-de la Torre O, Vázquez-Mahía I, Carral-Roura N, Rubín-Roger G, Penedo-Vázquez Á, Luaces-Rey R, López-Cedrún JL. Surgical management of ameloblastoma. Review of literature. *J Clin Exp Dent.* 2019 Jan 1;11(1):e70–e75. doi:10.4317/jced.55452
  9. Chakraborty S, Guha RP, Naskar S, Banerjee R. Custom-Made 3D Titanium Plate for Mandibular Reconstruction in Surgery of Ameloblastoma: A Novel Case Report. *Surgical Techniques Development.* 2022;11(3):98–104. doi.org/10.3390/std11030009
  10. Milman T, Ying GS, Pan W, LiVolsi V. Ameloblastoma: 25 Year Experience at a Single Institution. *Head Neck Pathol.* 2016 Dec;10(4):513–520. doi:10.1007/s12105-016-0734-5. Epub 2016 Jun 7.
  11. Ghai S. Ameloblastoma: An Updated Narrative Review of an Enigmatic Tumor. *Cureus.* 2022 Aug 6;14(8):e27734. doi:10.7759/cureus.27734
  12. Alves DBM, Tuji FM, Alves FA, Rocha AC, Santos-Silva ARD, Vargas PA, Lopes MA. Evaluation of mandibular odontogenic keratocyst and ameloblastoma by panoramic radiograph and computed tomography. *Dentomaxillofac Radiol.* 2018;47(7):20170288. doi:10.1259/dmfr.20170288
  13. Bispo MS, Pierre Júnior MLGQ, Apolinário AL Jr, Dos Santos JN, Junior BC, Neves FS, Crusoé-Rebello I. Computer tomographic differential diagnosis of ameloblastoma and odontogenic keratocyst: classification using a convolutional neural network. *Dentomaxillofac Radiol.* 2021 Oct 1;50(7):20210002. doi:10.1259/dmfr.20210002
  14. Apajalahti S, Kelppe J, Kontio R, Hagström J. Imaging characteristics of ameloblastomas and diagnostic value of computed tomography and magnetic resonance imaging in a series of 26 patients. *Oral Surg Oral Med Oral Pathol Oral Radiol.* 2015 Aug;120(2):e118–30. doi:10.1016/j.oooo.2015.05.002
  15. Laborde A, Nicot R, Wojcik T, Ferri J, Raoul G. Ameloblastoma of the jaws: Management and recurrence rate. *Eur Ann Otorhinolaryngol Head Neck Dis.* 2017 Feb;134(1):7–11. doi:10.1016/j.ano.2016.09.004
  16. Chana JS, Chang YM, Wei FC, Shen YF, Chan CP, Lin HN, Tsai CY, Jeng SF. Segmental mandibulectomy and immediate free fibula osteoseptocutaneous flap reconstruction with endosteal implants: an ideal treatment method for mandibular ameloblastoma. *Plast Reconstr Surg.* 2004 Jan;113(1):80–7. doi:10.1097/01.PRS.0000097719.69616.29
  17. Bataineh AB. Effect of preservation of the inferior and posterior borders on recurrence of ameloblastomas of the mandible. *Oral Surg Oral Med Oral Pathol Oral Radiol Endod.* 2000 Aug;90(2):155–63. doi:10.1067/moe.2000.107971
  18. Girardi GB, Arora K, Saifi AM. Ameloblastoma: A retrospective analysis of 31 cases. *J Oral Biol Craniofac Res.* 2017 Sep-Dec;7(3):206–211. doi:10.1016/j.jobcr.2017.08.007
  19. Gravvanis A, Koumoullis HD, Anterriotis D, Tsoutsos D, Katsikeris N. Recurrent giant mandibular ameloblastoma in young adults. *Head Neck.* 2016 Apr;38 Suppl 1:E1947–54. doi:10.1002/hed.24352
  20. Fuchigami T, Ono Y, Kishida S, Nakamura N. Molecular biological findings of ameloblastoma. *Jpn Dent Sci Rev.* 2021 Nov;57:27–32. doi:10.1016/j.jdsr.2020.12.003
  21. Hresko A, Burtyn O, Pavlovskiy L, Snisarevskiy P, Lapshyna J, Chepurniy Y, Kopchak A, Karagozolu KH, Forouzanfar T. Controversies in ameloblastoma management: evaluation of decision making, based on a retrospective analysis. *Med Oral Patol Oral Cir Bucal.* 2021 Mar 1;26(2):e181–e186. doi:10.4317/medoral.24104
  22. Pappalardo M, Tsao CK, Tsang ML, Zheng J, Chang YM, Tsai CY. Long-term outcome of patients with or without osseointegrated implants after resection of mandibular ameloblastoma and reconstruction with vascularized bone graft: Functional assessment and quality of life. *J Plast Reconstr Aesthet Surg.* 2018 Jul;71(7):1076–1085. doi:10.1016/j.bjps.2018.03.008
  23. Lonie S, Herle P, Paddle A, Pradhan N, Birch T, Shayan R. Mandibular reconstruction: meta-analysis of iliac – versus fibula-free flaps. *ANZ J Surg.* 2016 May;86(5):337–42. doi:10.1111/ans.13274
  24. Cariati G, Farhat MC, Dyalram D, Ferrari S, Lubek JE. The deep circumflex iliac artery free flap in maxillofacial reconstruction: a comparative institutional analysis. *Oral Maxillofac Surg.* 2021 Sep;25(3):395–400. doi:10.1007/s10006-020-00930-y
  25. Oteri G, Ponte FS, Pisano M, Cicciù M. Five years follow-up of implant-prosthetic rehabilitation on a patient after mandibular ameloblastoma removal and ridge reconstruction by fibula graft and bone distraction. *Dent Res J (Isfahan).* 2012 Mar;9(2):226–32. doi:10.4103/1735-3327.95241
  26. Tarsitano A, Sgarzani R, Betti E, Oranges CM, Contedini F, Cipriani R, Marchetti C. Vascular pedicle ossification of free fibular flap: is it a rare phenomenon? Is it possible to avoid this risk? *Acta Otorhinolaryngol Ital.* 2013 Oct;33(5):307–10.
  27. Wolff KD, Hölzle F, Kolk A, Hohlweg-Majert B, Steiner T, Kesting MR. Raising the osteocutaneous fibular flap for oral reconstruction with reduced tissue alteration. *J Oral Maxillofac Surg.* 2011 Jun;69(6):e260–7. doi:10.1016/j.joms.2010.11.040
  28. Piotrowska-Seweryn A, Szymczyk C, Walczak DA, Krakowczyk Ł, Maciejewski A, Hadasik G, Wierzgoń J, Szumniak R, Drozdowski P, Paul P, Grajek M. Fibular Free Flap and Iliac Crest Free Flap Mandibular Reconstruction In Patients With Mandibular Ameloblastomas. *J Craniofac Surg.* 2022 Oct 1;33(7):1962–1970. doi:10.1097/SCS.00000000000008524
  29. Sannomiya EK, Silva JV, Brito AA, Saez DM, Angelieri F, Dalben Gda S. Surgical planning for resection of an ameloblastoma and reconstruction of the mandible using a selective laser sintering 3D biomodel. *Oral Surg Oral Med Oral Pathol Oral Radiol Endod.* 2008 Jul;106(1):e36–40. doi:10.1016/j.tripleo.2008.01.014
  30. Yu Y, Zhang WB, Wang Y, Liu XJ, Guo CB, Peng X. A Revised Approach for Mandibular Reconstruction With the Vascularized Iliac Crest Flap Using Virtual Surgical Planning and Surgical Navigation. *J Oral Maxillofac Surg.* 2016 Jun;74(6):1285.e1–1285.e11. doi:10.1016/j.joms.2016.02.021
  31. Shu DL, Liu XZ, Guo B, Ran W, Liao X, Zhang YY. Accuracy of using computer-aided rapid prototyping templates for mandible reconstruction with an iliac crest graft. *World J Surg Oncol.* 2014 Jun 24;12:190. doi:10.1186/1477-7819-12-190
  32. Mazzola F, Smithers F, Cheng K, Mukherjee P, Hubert Low TH, Ch'ng S, Palme CE, Clark JR. Time and cost-analysis of virtual surgical planning for head and neck reconstruction: A matched pair analysis. *Oral Oncol.* 2020 Jan;100:104491. doi:10.1016/j.oraloncology.2019.104491